Rock and Soil Mechanics

Volume 41 | Issue 8 Article 7

1-22-2021

A study on the rainfall infiltration of granite residual soil slope with an improved Green-Ampt model

Yong-liang PAN

Wen-xing JIAN

Lin-jun LI

Yu-qiu LIN

See next page for additional authors

Custom Citation

PAN Yong-liang, JIAN Wen-xing, LI Lin-jun, LIN Yu-qiu, TIAN Peng-fei. A study on the rainfall infiltration of granite residual soil slope with an improved Green-Ampt model[J]. Rock and Soil Mechanics, 2020, 41(8): 2685-2692.

A study on the rainfall infiltration of granite residual soil slope with an improved Green-Ampt model

Authors

Yong-liang PAN, Wen-xing JIAN, Lin-jun LI, Yu-qiu LIN, and Peng-fei TIAN

Rock and Soil Mechanics 2020 41(8): 2685−2692 ISSN 1000−7598
https: //doi.org/10.16285/j.rsm.2019.6734 rocksoilmech.researchcommons.org/journal

A study on the rainfall infiltration of granite residual soil slope with an improved Green-Ampt model

PAN Yong-liang, JIAN Wen-xing, LI Lin-jun, LIN Yu-qiu, TIAN Peng-fei
Faculty of Engineering, China University of Geosciences(Wuhan),Wuhan, Hubei 430074, China

Abstract: Granite residual soil is widely distributed in southern China, and it has many poor physical and mechanical properties. Slopes of this type of soil are prone to deformation and failure under the action of rainfall. Therefore, it is of great significance to study the rainfall infiltration mechanism in granite residual soil slopes. On the basis of Green-Ampt model, the initial moisture content, underground water level and unsaturated characteristics of the soil are comprehensively considered. An infiltration model suitable for different rainfall conditions is established, and verified by comparison between numerical simulations and other models. Then, the proposed model is used to analyze granite residual soil slopes under three typical rainfall conditions. The results show that the initial water content has little effect on the migration rate of the wetting front when it is far from groundwater level, whereas the migration rate increases gradually when the wetting front is near groundwater level, presenting an exponential trend. In the same rainfall time, under the condition that the rainfall intensity is slightly greater than the saturated permeability coefficient of soil, the wetting front migration depth is the largest and the slope stability factor decreases the most.

Keywords: Green-Ampt infiltration model; wetting front; initial water content; rainfall condition; slope stability

1 Introduction

Rainfall is one of the most important environmental factors that induces landslides, and its disaster mechanism and process have always been the focus and difficulty of research. For soil slopes, the sliding surface often appears around the position of wetting front. It is of great significance for the prediction and prevention of landslides to study the migration mechanism of wetting front under rainfall. A large amount of studies have been carried out to establish the rainfall infiltration models, which varies significantly from each other. Some most common models of rainfall infiltration include Green-Ampt model, Mein-Larson model, Philips model, Richard model, etc. Particularly, due to its simple principle and convenient solution, the Green-Ampt model has been widely applied in the study of rainfall infiltration.

Mallari et al.[1] compared and analyzed the applicability of Horton and Green-Ampt infiltration models in slope flow, and concluded that compared with the Horton equation, the Green-Ampt equation could more accurately describe the advance moisture content conditions and flow process in soil. Wang et al.[2] combined the Green-Ampt model with the law of conservation of mass, and established a rainfall infiltration model considering the vertical and parallel seepage flow on the slope surface. Sajjan et al.[3] calculated the rainfall runoff of an embankment slope by using the Green-Ampt model and explicit finite difference method based on the Saint Venant continuity and momentum equation of surface runoff. Yao et al.[4] proposed SGA model to evaluate the slope rainfall infiltration process based on the concept of layered soil moisture content above the humid front. Gavin et al.[5] assumed that the matric suction of soil mass increases linearly with the depth after rainfall, and improved the Green-Ampt model. Tsai et al.[6] conducted permeability tests on sandy soils with different particle sizes, and based on the traditional Green-Ampt model, a dynamic effect MGAM infiltration model considering the capillary pressure was established.

Li et al.[7] improved the Mein-Larson rainfall infiltration model by using unsaturated soil VG model and Green-Ampt model, and further proposed a calculation model of rainfall-induced shallow landslide. Based on the Green-Ampt model, Jian et al.[8] presented a rainfall infiltration model under the influence of lower rainfall intensity considering the slope dip angle. Tong[9] deduced the landslide rainfall infiltration model applicable to the Three Gorges reservoir area under different rainfall conditions on the basis of the Green-Ampt model. Ma[10] introduced closed air pressure into slope stability analysis, and modified the classical Green-Ampt model to be applicable for heavy rainfall. Shi et al.[11] proposed a method for calculating the rainfall infiltration depth and for the stability analysis of multi-layer unsaturated soil slope with unequal thickness, and discussed the influence of different rainfall intensity and time on the slope stability. Tang et al. [12] improved the Green- Ampt model and showed that the initial water content of the slope body has a certain degree of influence on the rainfall infiltration process of landslides.

The analysis of the existing research results shows that many scholars regard the initial water content as an average value in order to improve the rainfall infil-

Received: 9 October 2019 Revised: 13 January 2020
This work was supported by the Science and Technology Program of Jiangxi Provincial Transportation Department (2015C0026) and the Open Fund Project of China University of Geosciences (Wuhan) Teaching Laboratory (SKJ2018099).
First author: Pan Yong-liang, male, born in 1995, Postgraduate students, mainly engaged in the research on engineering geology and geotechnical engineering. E-mail: 934732201@qq.com

tration model. This assumption is obviously inconsistent with the actual situation. The change of the initial water content will cause the changes of the migration rate of wetting front and of the slop stability coefficient. In this regard, Zhang et al. [13] determined the initial water content at different depths of the slope by matric suction, and deduced the rainfall infiltration model under the condition of non-uniformly distributed initial water content. However, the calculation process is relatively complex. Jian et al.[14] deduced a non- ponding rainfall infiltration model of shallow landslide in the form of exponential initial water content, which simplified the calculation process, but they did not discuss other rainfall conditions. Liu et al.[15] assumed that the initial water content of the slope body was linearly distributed and improved the Green-Ampt model, but the applicable conditions were limited.

In view of these shortcomings, this paper systematically improves the Green-Ampt model by comprehensively considering the non-uniformity of initial water content and multiple rainfall conditions. The proposed model can reflect the rainfall infiltration mechanism under natural conditions as far as possible, and further expands the engineering applicability.

The southern region of Jiangxi Province is rainy and is regarded as the center of China's rainstorm. Moreover, a large amount of granite residual soil is distributed, which has poor gradation, large pore ratio and easy disintegration when exposed to water[16]. According to the geological hazard survey and zoning data in Jiangxi Province, the soil landslides account for 91.4% of the 5758 landslides survey [17]. Therefore, the study of rainfall infiltration mechanism and stability of granite residual soil slope has great significance for the region.

2 Improvement of infiltration model based on Green-Ampt model

Green and Ampt's infiltration model based on the infiltration of thin layer ponding in soil has the expression as follows:

$$i(t) = K_s(1 + \frac{s_f + H}{z_f}) \quad (1)$$

where $i(t)$ is the infiltration rate at time t; K_s is the saturation permeability; z_f is the wetting front depth; s_f is the matric suction at the wetting front; and H is the depth of ponding.

The model assumes that the ground is horizontal, while the surface of the slope is inclined and the soil above the wetting front is not completely saturated. According to the investigation data, the initial water content of soil is not uniformly distributed with depth. Basically, the soil water content under natural conditions shows a trend of increase from slope surface to groundwater level. According to Godt et al.[18], in the case of monolayer soil, the distribution of soil water content is approximately a linearly-exponential curve. According to literatures [14] and [19–20], the distribution of soil water content can be described by an exponential function:

$$\theta_z = \theta(z_f) = \frac{\theta_s}{(d + 1 - z_f)^b} \quad (2)$$

where $\theta(z_f)$ is the soil water content distribution function in the direction of vertical slope surface; d is the depth of groundwater (m); θ_s is saturated water content (%); and b is the fitting parameter, which is related to the distribution of soil particles and pores.

The expression is simple in form and convenient for application in actual projects. The Green-Ampt infiltration model can be combined with the Eq.(2) to analyze the rainfall infiltration mechanism under different rainfall conditions. A schematic diagram of the rainfall infiltration mechanism is shown in Fig. 1, where q is rainfall intensity and β is slope dip angle.

2.1 Weak rainfall and non-ponding infiltration model

When the rainfall intensity is less than the saturated permeability of soil (as shown in Fig. 2), it is non-ponding infiltration, and the normal infiltration rate perpendicular to the slope surface is

$$i(t) = q\cos\beta \quad (3)$$

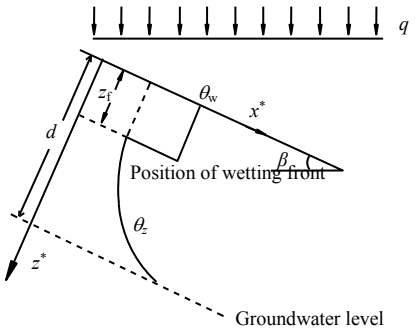

Fig. 1 Calculation diagram of rainfall infiltration

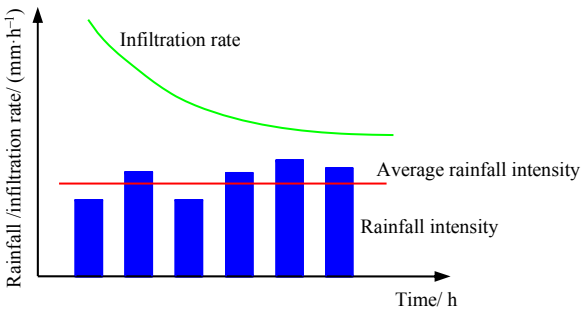

Fig. 2 Non-ponding infiltration condition of weak rainfall

According to the principle of water balance of the Green-Ampt model, the quantity of normal rainfall infiltration is equal to the increment of the water content in the normal direction. It is assumed that all rainfall will penetrate into the soil, and the volumetric water content of the soil at the wetting front is θ_w. The relationship between the rainfall infiltration and the depth of the wetting front can be express as

$$I=(\theta_s-\theta_z)z_f$$

$$[\theta_w-\theta_z]\mathrm{d}z_f=q\cos\beta\mathrm{d}t \tag{4}$$

$$\int[\theta_w-\frac{\theta_s}{(d+1-z_f)^b}]\mathrm{d}z_f=qt\cos\beta+c$$

In Eq.(4), c is a constant. Substituting the initial condition that $z_f=0$ when t=0 into Eq.(4), the following expression can be obtained by the integral calculation

$$t=\frac{\theta_w z_f(1-b)+\theta_s(d+1-z_f)^{1-b}-\theta_s(d+1)^{1-b}}{q(1-b)\cos\beta} \tag{5}$$

Equation (5) is the modified expression of the wetting front changing with time under the condition of weak rainfall intensity and non-ponding infiltration.

2.2 Heavy rainfall and ponding infiltration model

When the rainfall intensity is larger than the saturated permeability of the soil (as shown in Fig. 3), the permeability is mainly controlled by the permeability of soil itself, which can be regarded as the velocity of water flow in the soil.

According to Darcy's law, the permeability in this case is

$$i(t)=K_s\frac{z_f\cos\beta+s_f+H}{z_f} \tag{6}$$

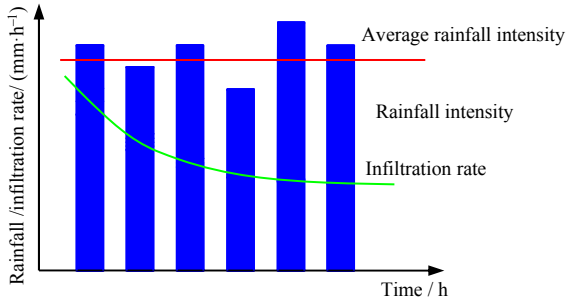

Fig. 3 Ponding infiltration conditions of heavy rainfall

where K_s is the saturated permeability coefficient of soil; and H is the depth of ponding on the slope, which can be regarded as 0 for steep slope.

Similarly

$$i(t)=\frac{\mathrm{d}I}{\mathrm{d}t}=\frac{(\theta_s-\theta_z)\mathrm{d}z_f}{\mathrm{d}t} \tag{7}$$

Therefore:

$$[\theta_w-\theta_z]\mathrm{d}z_f=i(t)\mathrm{d}t$$

$$\int[\theta_w-\frac{\theta_s}{(d+1-z_f)^b}]\mathrm{d}z_f=K_s\frac{z_f\cos\beta+s_f}{z_f}t+c \tag{8}$$

Substituting the initial condition that $z_f=0$ when $t=0$ into Eq.(8), the following integral can be obtained

$$t=\frac{[\theta_w z_f(1-b)+\theta_s(d+1-z_f)^{1-b}-\theta_s(d+1)^{1-b}]z_f}{K_s(z_f\cos\beta+s_f)(1-b)} \tag{9}$$

Equation (9) is the modified expression in the condition of heavy rainfall intensity and ponding infiltration.

2.3 Non-ponding to ponding conversion infiltration model

When the rainfall intensity is slightly greater than the saturated permeability of soil, as shown in Fig. 4, the infiltration rate before the occurrence of ponding infiltration can be obtained using Eq.(1), and the infiltration rate after ponding infiltration can be obtained using Eq. (3). There is a critical point from non-ponding infiltration to ponding infiltration. When ponding infiltration occurs, Eq.(1) and Eq.(3) are equal, that is

$$q\cos\beta=K_s\frac{z_f\cos\beta+s_f}{z_f} \tag{10}$$

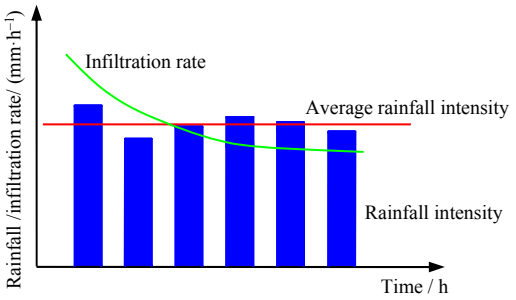

Fig. 4 Infiltration conditions with rainfall intensity slightly greater than saturation permeability coefficient

Suppose the critical wetting front depth is z_p; and the quantity of rainfall infiltration at the time of ponding is

$$I_p=\int_0^{z_p}[\theta_w-\frac{\theta_s}{(d+1-z)^b}]\mathrm{d}z \tag{11}$$

By simplifying and solving Eqs. (10) and (11), z_p and I_p are obtained as follows:

$$z_p=\frac{s_f}{q\cos\beta/K_s-\cos\beta} \tag{12}$$

$$I_p=\theta_s z_p+\theta_s\frac{(d+1-z_p)^{1-b}}{1-b} \tag{13}$$

Because

$$t_p=\frac{I_p}{q\cos\beta} \tag{14}$$

Thus

$$t_p=\frac{\theta_w z_p(1-b)+\theta_s(d+1-z_p)^{1-b}-\theta_s(d+1)^{1-b}}{q(1-b)\cos\beta} \tag{15}$$

That is, when $t<t_p$, it is the non-ponding infiltration stage, and the function expression is the same as the non-ponding infiltration process:

$$t=\frac{\theta_w z_f(1-b)+\theta_s(d+1-z_f)^{1-b}-\theta_s(d+1)^{1-b}}{q(1-b)\cos\beta} \tag{16}$$

When $t \geqslant t_p$, the integral expression is

$$\int(\theta_w - \frac{\theta_s}{(d+1-z_f)^b})\mathrm{d}z_f = t_p q\cos\beta + K_s\frac{z_f\cos\beta + s_f}{z_f}(t-t_p) + c \quad (17)$$

Substituting the initial condition that $z_f = z_p$ when $t = t_p$ into Eq. (17), the expression of c is obtained as follows:

$$c = \theta_w z_p + \frac{\theta_s(d+1-z_p)^{1-b}}{1-b} - t_p q\cos\beta \quad (18)$$

Therefore

$$t = t_p + \frac{z_f[\theta_w z_f(1-b) + \theta_s(d+1-z_f)^{1-b} - \theta_w z_p(1-b) - \theta_s(d+1-z_p)^{1-b}]}{K_s(z_f\cos\beta + s_f)(1-b)} \quad (19)$$

Equations (16) and (19) are the basic expressions of the whole process of non-ponding to ponding infiltration.

3 Rainfall infiltration law of granite residual soil slope in southern Jiangxi province

3.1 Verification of rainfall infiltration model

In southern Jiangxi Province where it is rainy all year round and the granite residual soil is widely distributed, the shallow landslides often occur. In this paper, an example slope was selected from the site of the Xiangtang Viaduct in the A1 section of Anyuan to Dingnan expressway in southern Jiangxi Province. The slope is 10 m high, 20 m wide, the natural inclination is 30° , and the groundwater table is 7 m in depth. The drilling data shows that the slope of more than 10 m is monzogranite residual soil. According to the comprehensive classification of granite residual soil proposed by Wu [21], this type of residual soil belongs to silty clay sand. The VG calculation parameters of the slope soil obtained from TRIM test are shown in Table 1, in which θ_r is residual volume water content and α and n are fitting parameters that related to the soil characteristics.

Table 1 Average value of VG calculation parameters for granite residual soil

θ_r	α	n	θ_s	K_s / (m • s^{-1})	S_f / cm
0.244	0.142	1.60	0.42	6.88×10^{-6}	8.14

According to the investigation data, the initial water content of soil at different depths can be obtained. According to Eq. (2), fitting results are shown in Fig.5, where R^2=0.978. Thus, the function relation of the initial water content with the change of depth can be obtained as follows:

$$\theta_z = \frac{0.435}{(8-z_f)^{0.303}} \quad (20)$$

In the actual rainfall condition, the soil above the wetting front cannot reach full saturation. In this paper, we assumed $\theta_w = 0.9\,\theta_s$ based on literature[22]. According to the data of Jiangxi Meteorological Service, three typical rainfall conditions, namely, 8 mm/h common rainfall intensity in the rainy season in southern Jiangxi Province, 26 mm/h rainfall intensity that slightly greater than the saturated permeability coefficient of soil and 50.8 mm/h maximum rainfall intensity in July 2018 in Dingnan County of Jiangxi Province, were selected for case studies, which were respectively set as working conditions 1, 2 and 3.

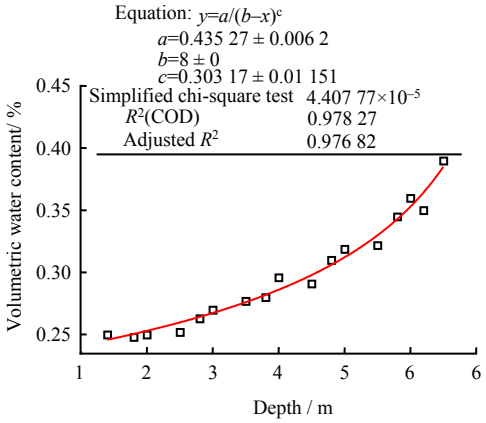

Fig. 5 Curve fitting of volumetric moisture content with depth

The model of Eq. (28) in literature [13] (Eq. (21) in this paper) is used for comparative verification. This model divides all the rainfall infiltration processes into two stages, i.e., the stages before and after ponding infiltration. The initial water content of the slope θ_z is regarded as uniformly distributed, which is 0.288 in this case. The permeability coefficient of the soil K_w is calculated as saturated permeability coefficient K_s according to the Green-Ampt model, as shown in Eq. (21):

$$t = \begin{cases} \dfrac{z_f(\theta_s-\theta_z)}{q\cos\beta} & t \leqslant t_p \\ t_p + \dfrac{(\theta_s-\theta_z)(z_f-z_p)}{K_w\cos\beta} - \dfrac{s_f(\theta_s-\theta_z)}{K_w\cos^2\beta} ln(\dfrac{z_f\cos\beta+s_f}{z_p\cos\beta+s_f}) & t > t_p \end{cases} \quad (21)$$

Next, Seep/W software is used for numerical simulation. The left and right sides of the slope are set to be impervious boundary, and the bottom to be unit gradient boundary. According to the magnitude of rainfall intensity, the corresponding unit flow boundary or pressure head boundary is applied to the slope surface as well as the top of the slope. The position of the wetting front

can be determined by defining the pore water pressure value. Here, the vertical distance from the top of the slope to the wetting front is taken as the migration depth of the wetting front.

The improved model in this paper, the model in literature [13], and the numerical simulation are respectively used for calculation, and the results are shown in Table 2. Through comparative studies, we can see that the calculation results of the improved Green-Ampt model in this paper are in good agreement with the other two validation results. It can also be seen that the infiltration depth at 24h calculated according to the method in literature [13] is slightly larger than that calculated by the improved model in this paper under conditions-1 and -3, but the final infiltration depth at 24h under the condition-2 is contrary to those mentioned above. This is mainly related to the assumption that the initial water content of soil at different depths of slope is the mean value, which is larger or smaller than the actual moisture content.

Table 2 The change of wetting front depth with different rainfall intensities over time

Rainfall intensity / (mm • h^{-1})	Types of calculation	Infiltration depth of wetting front /m							
		3 h	6 h	9 h	12 h	15 h	18 h	21 h	24 h
8.0	Improved model solution	0.190	0.323	0.460	0.593	0.738	0.880	1.024	1.167
	Model solution[13]	0.156	0.312	0.469	0.625	0.782	0.938	1.094	1.251
	Numerical solution	0.201	0.308	0.509	0.576	0.721	0.825	1.030	1.221
26.0	Improved model solution	0.557	1.13	1.65	2.24	2.65	3.24	3.81	4.46
	Model solution[13]	0.590	1.17	1.76	2.35	2.54	3.04	3.53	4.02
	Numerical solution	0.550	1.05	1.74	2.41	2.71	3.34	3.92	4.61
50.8	Improved model solution	0.552	0.998	1.45	1.93	2.32	2.87	3.45	4.05
	Model solution[13]	0.574	1.072	1.56	2.06	2.55	3.04	3.53	4.08
	Numerical solution	0.598	1.130	1.64	2.17	2.79	3.31	3.77	4.25

3.2 Analysis of rainfall infiltration law

The variation curves of wetting front depth with 30 h of continuous rainfall under the above three typical rainfall intensities are calculated according to the improved Green-Ampt model in this paper, as shown in Figs. 6–8. It can be seen from Fig. 6 that, under working condition-1, the migration rule of the wetting front basically changes linearly with time, which is due to the fact that the infiltration rate under this condition is mainly controlled by rainfall intensity. On the other hand, the rainfall intensity is small and the amount of infiltration is insuffIcient, indicating that the water needed for the wetting front to continue to move down is not satisfied. Therefore, the depth of infiltration is small. It can also be seen from Fig. 5 that the initial water content of soil close to slope surface varies little with depth, and the change of water content has little influence on the migration rate of the wetting front.

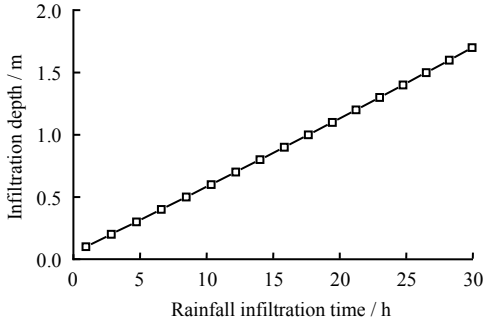

Fig. 6 Change of wetting front over time in working condition 1

When the rainfall intensity is greater than the saturated permeability of soil, such as under working conditions-2 and -3, the soil infiltration rate is mainly controlled by its own permeability characteristics, and the rainfall intensity can meet the increment of volumetric water content required by the continuous migration of the wetting front, therefore the infiltration depth is relatively large. Figure 7 shows the non-ponding to ponding infiltration rainfall condition with rainfall intensity of 26 mm/h. Based on the calculation of Eqs. (15) and (19), it can be seen that after rainfall of 12.59 h, when the migration depth of the wetting front reaches 2.36 m, there will be ponding infiltration after this point. Figures 7 and 8 present that when the infiltration depth is less than 3 m, the image approximately changes linearly, and when it is more than 3 m, it gradually shows an exponential change trend.

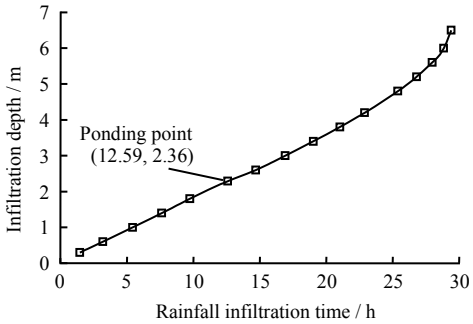

Fig. 7 Change of wetting front over time in working condition 2

By comparing the rainfall infiltration mechanisms under the three conditions, it can be found that the closer to the groundwater table, the steeper the curve, and the faster the migration rate of the wetting front. This is because the initial water content of the soil near the groundwater table is higher, and the increment of the volumetric water content required for the soil to reach saturation is also reduced. Thus, the time needed to move the same distance is shortened. In addition, the maximum migration depth of wetting front during the

same rainfall time is working condition-2, which is related to the larger average infiltration rate and sufficient water supply in the whole process under this condition.

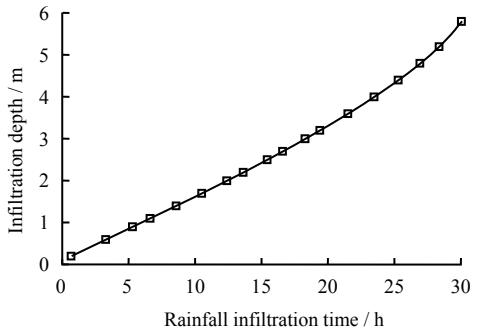

Fig. 8 Change of wetting front over time in working condition 3

3.3 Influence of rainfall on the stability of granite residual soil slope in southern Jiangxi

On one hand, rainfall will reduce the suction of slope soil matrix; on the other hand, it will produce softening and lubricating effect, which will reduce the soil cohesion and internal friction angle, thus reducing the sliding resistance and causing slope deformation and failure. In the soil slope, the sliding surface usually develops at the wetting front or the interface of different types of soil layers. Since the slope soil in this paper is silty clay sand, it is assumed that the slope has a plane sliding at the wetting front. The infinite slope limit equilibrium method is adopted to calculate the factor of safety (F_s) (see Fig. 9).

$$F_s = \frac{c' + (\gamma_s z_f \cos\beta + s_f \gamma_w)\tan\varphi'}{\gamma_s z_f \sin\beta} \quad (22)$$

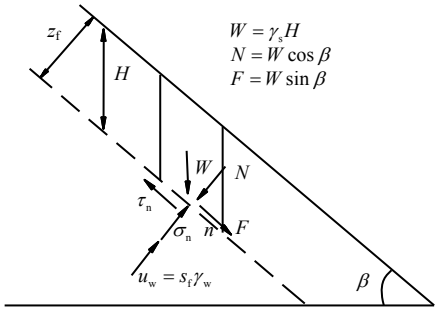

Fig. 9 Schematic of infinite slope stability analysis

where c' =5.70 kPa is the effective cohesion force; φ' =29.7° is the effective internal friction angle; and γ_s =18.08 kN/m^3 is the saturated unit weight of granite residual soil. According to the wetting front depth of continuous rainfall for 30 h under three rainfall intensities obtained above, the F_s of the slope at corresponding time was calculated, as shown in Figs. 10–12.

Figures 10–12 illustrate that as the wetting front migrates under the influence of rainfall, F_s decreases continuously. In the first 5 h, F_s drops the most, while after 30 h, F_s decreases by about 3.5–5 times compared with the initial rainfall. This is because with the infiltration of rain, the soil gradually changes from unsaturated to saturated, the matric suction gradually decreases, and the pore water pressure gradually increases. Meanwhile, the increase of water content also makes the sliding component of slope soil's selfweight increase correspondingly, and then the F_s value will be greatly reduced.

Comparing 3 kinds of rainfall conditions found that the F_s value decreases by a relatively small margin when the rainfall intensity is small (working condition-1, as shown in Fig.10); after 30 h of rainfall, F_s is equal to 1.394, which is regarded as a safe condition. With the increase of rainfall intensity, F_s also decreases rapidly. After 30 h, the F_s value of working condition-2 is 1.097 (see Fig.11), and that of working condition-3 is 1.115 (see Fig.12). It implies that the condition with rainfall intensity slightly larger than the saturated permeability coefficient is more likely to cause slope failure than the condition with rainfall intensity much larger than the saturated permeability coefficient, which is consistent with the variation of wetting front depth with time. Therefore, without considering the effect of rainfall scour on slope surface, when rainfall intensity exceeds a certain threshold, increasing rainfall intensity will not make the wetting front depth increase deeper and the F_s value decrease more in the same rainfall time.

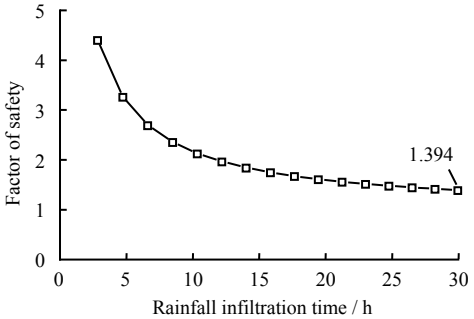

Fig. 10 Factor of safety over time with rainfall intensity of 8 mm/h

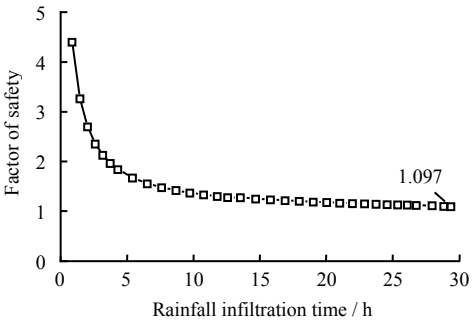

Fig. 11 Factor of safety over time with rainfall intensity of 26 mm/h

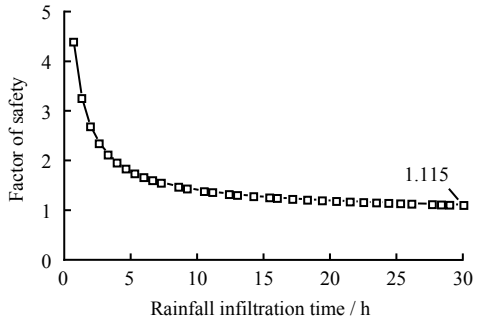

Fig. 12 Factor of safety over time with rainfall intensity of 50.8 mm/h

4 Conclusion

Based on the Green-Ampt model, a rainfall infiltration model for slope stability analysis considering the initial water content, groundwater level, and applicability to different rainfall conditions was established. The results of wetting front depth with time calculated by the proposed model were verified by other comparative models and numerical simulation, and were also in good agreement with the actual rainfall infiltration situation.

Focusing on granite residual soil slope in southern Jiangxi Province under three rainfall conditions, the variation of wetting front depth and slope factor of safety with time was analyzed. It was found that the wetting front depth changes linearly with time when it is near the slope surface and far away from the groundwater level. However, as the wetting front approaches the groundwater surface, the migration rate increases gradually, showing an exponential trend.

Under the three rainfall conditions, in the same rainfall time, the wetting front migration depth in the second condition was the largest, and the slope factor of safety also decreased the most. Therefore, for areas with a wide distribution of granite residual soil, it is particularly necessary to be vigilant for rainfall intensity slightly greater than saturated permeability coefficient, which poses the greatest threat to slope stability.

References

[1] MALLARI KRISTINE JOY B, ARGUELLES ANYA CATHERINE C, KIM HWANSUK HAFZULLAH AKSOY, et al. Comparative analysis of two infiltrationmodels for application In a physically based overland flow model[J]. Environmental Earth Sciences, 2015, 74(2): 1579–1587.

[2] WANG Ding-jian, TANG Hui-ming, ZHANG Ya-hui, et al. An improved approach for eva-luating the time-dependent stability of colluvial landsli-des during intense rainfall[J]. Environmental Earth Sciences, 2017, 76(8): 321.

[3] SAJJAN A K, GYASI-AGYEI Y, SHARMA R H. Rainfall runoff modelling of railway embankment steep slopes[J]. Hydrological Sciences Journal, 2013, 58(5): 1162–1176.

[4] YAO Wen-min, LI Chang-dong, ZHAN Hong-bin, et al. Time-dependent slope stabilityduring intense rain-fall with stratified soil water content[J]. Bulletin of Engineering Geology and the Environment, 2019, 78(7): 4805–4819.

[5] GAVIN Kenneth, XUE Jianfeng. A simple method to analyze infiltration into unsaturated soil slopes[J]. Computers and Geotechnics, 2008, 35(2): 223–230.

[6] TSAI Yi-zhih, LIU Yu-tung, WANG Yung-li, et al. Effects of the grain size on dynamic capillary pressure and the modified Green-Ampt model for infiltration[J]. Volume Geofluids, 2018, (2): 1–11.

[7] LI Ning, XU Jian-cong, QIN Ya-zhou. Research on calculation model for stability evaluation of rainfall induced shallow landslides[J]. Rock and Soil Mechanics, 2012, 33(5): 1485–1490.

[8] JIAN Wen-xing, XU Qiang, TONG Long-yun. Rainfall infiltration model of Huangtupo landslide in Three Gorges Reservoir area[J]. Rock and Soil Mechanics, 2013, 34(12): 3527–3533, 3548.

[9] TONG Long-yun. Rainfall infiltration process of huangtupo landslide in the Three Gorges Reservoir[D]. Wuhan: China University of Geosciences, 2013.

[10] MA Shi-guo. Study on the stability of infinite slop based on Green-Ampt infiltration model under intense rainfall[D]. Hangzhou: Zhejiang University, 2014.

[11] SHI Zhen-ming, SHEN Dan-yi, PENG Ming, et al. Slope stability analysis by considering rainfall infiltration in multilayered unsaturated soils[J]. Journal of Hydraulic Engineering, 2016, 47(8): 977–985.

[12] TANG Yang, YIN Kun-long, XIA Hui. Effects of initial water content on the rainfall infiltration and stability of shallow landslide[J]. Geological Science and Technology Information, 2017, 36(5): 204–208, 237.

[13] ZHANG Jie, LÜ Te, XUE Jian-feng, et al. Modified Green-Ampt model for analyzing rainfallinfiltration in slopes[J]. Rock and Soil Mechanics, 2016, 37(9): 2451–2457.

[14] JIAN Wen-xing, JIANG Yi. Exponential model of rainfall infitration of shallow landslides for nonponding conditions[J]. Safety and Environmental Engineering, 2017, 24(1): 22–25, 32.

[15] LIU Zi-zhen, YAN Zhi-xin, DUAN Jian, et al. Infiltration regulation and stability analysis of soilslope under sustained and small intensity rainfall[J]. Journal of Central South University, 2013, 20(9): 2519–2527.

[16] HU J Z, WANG H, MA J Z, et al. Probalilistic assessment of the properties of completely decomposed granite[C]// 6th Asian-Pacific Symposium on Structrural Reliability and Its Applications. Shanghai: [s. n.], 2016.

[17] BIAN Xiao-geng. The forming conditions frequent collapa and slide geological disaster in Jiangxi[J]. Yunnan Geology, 2016(3): 432–437.

[18] GODT JONATHAN W, ŞENER-KAYA BAŞAK, LU Ning, et al. Stability of infinite slopes under transient partially saturated seepage conditions[J]. Water Resources Reserch, 2012, 48(5): W05505.

[19] CHEN Hong-song, SHAO Ming-an, WANG Ke-lin. Effects of initial water content on hillslope rainfall infiltration and soil water redistribution[J]. Transactions of the Chinese Society of Agricultural Engineering, 2006, 22(1): 44–47.

[20] WANG Yun-qiang, ZHANG Xing-chang, CONG Wei, et al. Spatial variability of soil moisture on slope-land under-different land uses on the loess plateau[J]. Transactions of the Chinese Society of Agricultural Engi- neering, 2006, 22(12): 65–71.

[21] WU Neng-sen. Study on classification of granite residual soils[J]. Rock and Soil Mechanics, 2006, 27(12): 2299–2305.

[22] NG C W W, SHI Q. A numerical investigation of the stability of unsaturated soil slopes subjected to transient-seepage[J]. Computer and Geotechnics, 1998, 22(1): 1–28.